

2022-07-05

Bi-allelic variants in WNT7B disrupt the development of multiple organs in humans

Baptista, Julia

<http://hdl.handle.net/10026.1/19357>

10.1136/jmedgenet-2022-108475

Journal of Medical Genetics

BMJ Publishing Group

All content in PEARL is protected by copyright law. Author manuscripts are made available in accordance with publisher policies. Please cite only the published version using the details provided on the item record or document. In the absence of an open licence (e.g. Creative Commons), permissions for further reuse of content should be sought from the publisher or author.

Journal of Medical Genetics

Bi-allelic variants in *WNT7B* disrupt the development of multiple organs in humans

Journal:	<i>Journal of Medical Genetics</i>
Manuscript ID	jmedgenet-2022-108475.R2
Article Type:	Original research
Date Submitted by the Author:	n/a
Complete List of Authors:	<p>Bouasker, Samir; University Hospital Centre Sainte-Justine Patel, Nisha; King Faisal Specialist Hospital and Research Center, Department of Translational Genomics, Center for Genomic Medicine Greenlees, Rebecca; Westmead Institute for Medical Research Wellesley, Diana; Southampton University Hospitals NHS Trust Fares-Taie, Lucas; Imagine Institute for Genetic Diseases Almontashiri, Naif ; Taibah University Baptista, Julia; Royal Devon and Exeter NHS Foundation Trust Alghamdi, Malak ; King Saud University College of Medicine Boissel, Sarah; University Hospital Centre Sainte-Justine, Université de Montréal Martinovic, Jelena; Hopital Antoine-Beclere Prokudin, Ivan; Westmead Institute for Medical Research Holden, Samantha; Southampton University Hospitals NHS Trust Mudhar, Hardeep-Singh; Royal Hallamshire Hospital Histopathology Department Riley, Lisa ; Westmead Institute for Medical Research Nassif, Christina; University Hospital Centre Sainte-Justine, Université de Montréal ATTIE-BITACH, Tania; Necker-Enfants Malades Hospitals, Genetics Miguet, Marguerite; University Hospital Centre Sainte-Justine Delous, Marion; Université Lyon 1 Faculté de Médecine Lyon-Est Ernest, Sylvain; Imagine Institute for Genetic Diseases Plaisancie, Julie; Hospital Purpan Calvas, Patrick; Hospital Purpan, Department of Medical Genetics Rozet, Jean-Michel; Imagine Institute for Genetic Diseases Khan, Arif; Cleveland Clinic Abu Dhabi, pediatric ophthalmology Hamdan, Fadi; University Hospital Centre Sainte-Justine, Université de Montréal Jamieson, Robyn; Westmead Institute for Medical Research, Eye & Developmental Genetics Research Group Alkuraya, Fowzan; King Faisal Specialist Hospital and Research Center, Department of Translational Genomics, Center for Genomic Medicine; Alfaisal University, Department of Anatomy and Cell Biology Michaud, Jacques L.; CHU Sainte-Justine, ; Université de Montréal, Departments of Pediatrics and Neurosciences Chassaing, Nicolas; Hospital Purpan, Department of Medical Genetics</p>
Keywords:	Human Genetics

1
2
3
4
5
6
7
8
9
10
11
12
13
14
15
16
17
18
19
20
21
22
23
24
25
26
27
28
29
30
31
32
33
34
35
36
37
38
39
40
41
42
43
44
45
46
47
48
49
50
51
52
53
54
55
56
57
58
59
60



SCHOLARONE™
Manuscripts



I, the Submitting Author has the right to grant and does grant on behalf of all authors of the Work (as defined in the below author licence), an exclusive licence and/or a non-exclusive licence for contributions from authors who are: i) UK Crown employees; ii) where BMJ has agreed a CC-BY licence shall apply, and/or iii) in accordance with the terms applicable for US Federal Government officers or employees acting as part of their official duties; on a worldwide, perpetual, irrevocable, royalty-free basis to BMJ Publishing Group Ltd ("BMJ") its licensees and where the relevant Journal is co-owned by BMJ to the co-owners of the Journal, to publish the Work in this journal and any other BMJ products and to exploit all rights, as set out in our [licence](#).

The Submitting Author accepts and understands that any supply made under these terms is made by BMJ to the Submitting Author unless you are acting as an employee on behalf of your employer or a postgraduate student of an affiliated institution which is paying any applicable article publishing charge ("APC") for Open Access articles. Where the Submitting Author wishes to make the Work available on an Open Access basis (and intends to pay the relevant APC), the terms of reuse of such Open Access shall be governed by a Creative Commons licence – details of these licences and which [Creative Commons](#) licence will apply to this Work are set out in our licence referred to above.

Other than as permitted in any relevant BMJ Author's Self Archiving Policies, I confirm this Work has not been accepted for publication elsewhere, is not being considered for publication elsewhere and does not duplicate material already published. I confirm all authors consent to publication of this Work and authorise the granting of this licence.

Bi-allelic variants in *WNT7B* disrupt the development of multiple organs in humans.

Samir Bouasker, PhD¹, Nisha Patel, PhD², Rebecca Greenlees, BSc, PhD³, Diana Wellesley, MD⁴, Lucas Fares Taie, PhD⁵, Naif A Almontashiri, Ph.D^{6,7}, Júlia Baptista, PhD^{8,9}, Malak Ali Alghamdi, MD¹⁰, Sarah Boissel, PhD¹, Jelena Martinovic, MD¹¹, Ivan Prokudin, BSc, PhD³, Samantha Holden, MD¹², Hardeep-Singh Mudhar, FRCPath, PhD¹³, Lisa G. Riley, BSc, PhD^{14,15}, Christina Nassif, MSc¹, Tania Attie-Bitach, MD, PhD^{16,17}, Marguerite Miguet, MD¹, Marion Delous, PHD¹⁸, Sylvain Ernest, PhD¹⁶, Julie Plaisancié, MD^{19,20,21}, Patrick Calvas, MD, PhD^{19,20}, Jean-Michel Rozet, PhD⁵, Arif O. Khan, MD²², Fadi H. Hamdan, MSc, PhD¹, Robyn V. Jamieson, PhD, FRACP^{3,23}, Fowzan S. Alkuraya, MD^{2,24} Ω^* , Jacques L. Michaud, MD^{1,25} Ω^* , Nicolas Chassaing, MD, PhD^{19,20} Ω^*

¹Research Center, CHU Sainte-Justine, Montreal, H3T 1C5, Canada
²Department of Translational Genomics, Center for Genomic Medicine, King Faisal Specialist Hospital and Research Center, Riyadh 11211, Saudi Arabia
³Eye Genetics Research Unit, Children's Medical Research Institute, University of Sydney; The Children's Hospital at Westmead, Sydney Children's Hospitals Network; and Save Sight Institute, Sydney, New South Wales, Australia
⁴Wessex Clinical Genetic Service, University Hospital Southampton, Southampton, UK
⁵Laboratory Genetics in Ophthalmology, INSERM UMR1163-Institute of Genetic Diseases, Imagine, Université Paris Descartes-Sorbonne Paris Cité, 24 Boulevard du Montparnasse, 75015, Paris, France
⁶Center for Genetics and Inherited Diseases (CGID), Taibah University, Medina, Saudi Arabia
⁷Research Department, King Khaled Eye Specialist Hospital, Riyadh, Saudi Arabia.
⁸Peninsula Medical School, Faculty of Health, University of Plymouth, UK
⁹Institute of Biomedical and Clinical Science, University of Exeter Medical School, Exeter, UK
¹⁰Medical Genetic Division, Pediatric Department, College of Medicine, King Saud University, Riyadh, Saudi Arabia
¹¹APHP, Unit of Fetal Pathology, Antoine Bécclère Hospital, 92140 Clamart, France
¹²Department of Cellular Pathology, University Hospital Southampton, Southampton, UK
¹³ National Specialist Ophthalmic Pathology Service (NSOPS), Dept of Histopathology, Royal Hallamshire Hospital, Sheffield, England UK
¹⁴Rare Diseases Functional Genomics Laboratory, The Children's Hospital at Westmead, Sydney Children's Hospitals Network; Children's Medical Research Institute, University of Sydney, Sydney, New South Wales, Australia.

¹⁵Specialty of Paediatrics and Child Health, Faculty of Medicine and Health, University of Sydney, Sydney, New South Wales, Australia

¹⁶Laboratory of Embryology and Genetics of Congenital Malformations, INSERM UMR 1163, Imagine Institute, Paris, France

¹⁷SoFFoet (French Society of Foetopathology)

¹⁸Equipe GENDEV, Centre de Recherche en Neurosciences de Lyon, Inserm U1028, CNRS UMR5292, Université Lyon 1, Université St Etienne, Lyon, France

¹⁹Department of Medical Genetics, Purpan University Hospital, Toulouse, France

²⁰Centre de Référence des Affections Rares en Génétique Ophtalmologique CARGO, Site Constitutif, CHU Toulouse, Toulouse, France

²¹INSERM U1214, ToNIC, Université Toulouse III, Toulouse, France

²²Eye Institute, Cleveland Clinic Abu Dhabi, Abu Dhabi, United Arab Emirates

²³Specialty of Genomic Medicine, Faculty of Medicine and Health and Child and Adolescent Health, University of Sydney, Sydney, New South Wales, Australia

²⁴Department of Anatomy and Cell Biology, College of Medicine, Alfaisal University, Riyadh 11533, Saudi Arabia

²⁵Departments of Pediatrics and Neurosciences, Université de Montréal, Montreal, H3T 1J4, Canada

^ΩThese authors contributed equally to this work.

***Corresponding authors:**

Jacques L. Michaud, CHU Sainte-Justine Research Center, 3175 Côte Sainte-Catherine, Montréal, Qc, Canada H3T 1C5; e-mail: jacques.michaud.med@ssss.gouv.qc.ca; phone : 1-514-345-4931, ext: 4740

Nicolas Chassaing, Service de Génétique Médicale, Hôpital Purpan, Place du Dr Baylac, 31059 Toulouse, France; e-mail: chassaing.n@chu-toulouse.fr; phone : +33 5 61 77 90 51

Fowzan S. Alkuraya, Department of Genetics, King Faisal Specialist Hospital and Research Center, Riyadh 11211, Saudi Arabia; e-mail: FAIKuraya@kfshrc.edu.sa ; phone : (+96611) 464-7272

ABSTRACT

Background: Pulmonary hypoplasia, Diaphragmatic anomalies, Anophthalmia/Microphthalmia, and Cardiac defects delineate the PDAC syndrome. We aim to identify the cause of PDAC syndrome in patients who do not carry pathogenic variants in *RARB* and *STRA6*, which have been previously associated with this disorder.

Methods: We sequenced the exome of patients with unexplained PDAC syndrome and performed functional validation of candidate variants.

Results: We identified bi-allelic variants in *WNT7B* in fetuses with PDAC syndrome from two unrelated families. In one family, the fetus was homozygous for the c.292C>T (p.(Arg98*)) variant whereas the fetuses from the other family were compound heterozygous for the variants c.225C>G (p.(Tyr75*)) and c.562G>A (p.(Gly188Ser)). Finally, a molecular autopsy by proxy in a consanguineous couple that lost two babies due to lung hypoplasia revealed that both parents carry the p.(Arg98*) variant. Using a WNT signaling canonical luciferase assay, we demonstrated that the identified variants are deleterious. In addition, we found that *wnt7bb* mutant zebrafish display a defect of the swimbladder, an air-filled organ that is a structural homolog of the mammalian lung, suggesting that the function of WNT7B has been conserved during evolution for the development of these structures.

Conclusion: Our findings indicate that defective WNT7B function underlies a form of lung hypoplasia that is associated with the PDAC syndrome, and provide evidence for involvement of the WNT- β -catenin pathway in human lung, tracheal, ocular, cardiac, and renal development.

Key words: *WNT7B*, microphthalmia, lung agenesis, tracheomalacia, diaphragmatic eventration, cardiac defect, hypoplastic kidneys, PDAC syndrome, Matthew-Wood syndrome

KEY MESSAGES

What is already known on this topic: The combination of Pulmonary hypoplasia/agenesis, Diaphragmatic hernia/eventration, Anophthalmia, and Cardiac defects delineates the PDAC syndrome. Pathogenic variants in two genes involved in the retinoic acid pathway, *STRA6* and *RARB*, were previously known to be involved in this syndrome but explained only a subset of cases.

What this study adds: We identified *WNT7B* bi-allelic pathogenic variants in one newborn and two fetuses, from two families, displaying features overlapping with the PDAC syndrome. In a third family, molecular autopsy by proxy in a couple that lost two babies due to lung hypoplasia revealed that both parents were heterozygous for a *WNT7B* nonsense variation.

How this study might affect research, practice or policy: This study identified a third PDAC syndrome gene and raises the possibility that PDAC syndrome involves developmental processes that are regulated by an interaction between the retinoic acid and WNT pathways.

INTRODUCTION

Pulmonary agenesis is a congenital anomaly in which there is complete absence or severe hypoplasia of one or both lungs, estimated to complicate around 1 per 15,000 pregnancies.¹ Very little is known about its genetic basis in humans. Moreover, even if up to 50% of fetuses or newborns with pulmonary agenesis have associated congenital abnormalities,¹ there are very few recognizable syndromes associated with this developmental anomaly. The combination of Pulmonary hypoplasia/agenesis, Diaphragmatic hernia/eventration, Anophthalmia, and Cardiac defects delineates one such syndrome: the PDAC syndrome, also known as Matthew-Wood syndrome (MWS), Spear syndrome or MCOPS9 (MIM 601186). Pathogenic variants in two genes, namely *STRA6* (MIM 610745; autosomal recessive inheritance) and *RARB* (MIM 615524; autosomal dominant and recessive inheritance) have previously been identified in PDAC-affected individuals.^{2,3} Many cases of PDAC syndrome, however, remain unexplained.

By using exome sequencing (ES), we identified biallelic likely deleterious variants in *WNT7B* in 3 families with phenotypes consistent with PDAC syndrome. In order to confirm the link between *WNT7B* pathogenic variants, we studied *wnt7ba* and *wnt7bb* mutant zebrafish lines. We finally developed *in vitro* functional analyses to confirm the deleterious effect of the identified variants in our patients. Our results suggest that bi-allelic variants in *WNT7B* cause a polymalformative disorder that overlaps with the PDAC syndrome.

METHODS

Patients and molecular screening

We first performed ES in three patients with features of the PDAC syndrome (patients 1 to 3). To identify potentially pathogenic variants in exomes, we filtered out synonymous variants, intronic variants other than those affecting the consensus splice sites, and variants with a minor allele frequency greater than 0.5% in public (1000 Genomes, EVS, dbSNP138, GnomAD) and local (CHU Sainte-Justine Research Center exome dataset) databases. We next query variants affecting the same genes within the 3 screened individuals, as *de novo*, homozygous and compound heterozygous variants for each individual.

Seventeen additional patients (patients 4 to 20) with features of the PDAC syndrome and no identified pathogenic variants in *STRA6* and *RARB* were also screened by Sanger sequencing of all *WNT7B* coding exons using the primers listed in Table S1 (patients 4 to 20). Finally, four patients from two families were identified by GeneMatcher⁴ as they harbor rare variants in *WNT7B* (Patients 21 to 24). In these families, molecular screening was performed by ES for patient 21 and the parents of patients 23 and 24. Sanger sequencing was used to investigate the presence of the familial variants in patient 22. Phenotype of these 24 patients are summarized in Table S2. Variants numbering refers to the NM_058238.2 *WNT7B* isoform.

Study of *wnt7ba* and *wnt7bb* mutant zebrafish lines

The zebrafish genome contains two orthologs of *WNT7B*, *wnt7ba* and *wnt7bb*, whose corresponding proteins share an identity of 85 % and 89 %, respectively, with their human homolog.⁵ The *wnt7ba* (sa31394) and *wnt7bb* (sa24585) mutant zebrafish lines were generated at

the Wellcome Trust Sanger Institute (Stemple Laboratory) and obtained from the European Zebrafish Resource Center (EZRC) of the Karlsruhe Institute of Technology (KIT). The *wnt7ba* and *wnt7bb* lines harbour a nonsense point mutation at exon 2 (XM_686786.6: c.154C>T; p.(Gln52*)) and exon 3 (XM_017354279.2: c.517A>T; p.(Lys177*)), respectively.

Adult zebrafish (7-9 months old) were analysed by X-ray and histological analysis. Fishes were sacrificed by prolonged immersion (10 min) in Benzocaine, (375µg/l) and X-rayed using a Faxitron (MX-20DC12). Whole fish were fixed overnight in 4% paraformaldehyde at 4°C, decalcified in a 0.5 M EDTA pH 8.0 solution for 10 days at 4°C and embedded in paraffin. Cross (head) or coronal (body) sections of 4 µm were stained with hematoxylin–eosin (H&E ; eyes and heart) or Periodic acid-Schiff (PAS ; kidney).

Functional analyses

In vitro functional analysis. *WNT7B* cDNA was cloned into the pCMV-SPORT6 vector (Invitrogen) in frame with a green fluorescent protein (*gfp*) cassette. Site-directed mutagenesis (Invitrogen) was used to introduce the variants into the *WNT7B* cDNA. HEK293T cells were plated to 60 to 80 % confluency in 96-well plates and subsequently transfected with plasmids expressing *WNT7B* (WT or mutant; 75 ng), *Renilla* luciferase (125 pg), TOPFlash/FOPFlash (25 ng) and LRP5 (25 ng). LRP5 cooperatively activates canonical Wnt signaling with *WNT7B*.⁶ Luciferase activity was assayed 24 hours after transfection, using a dual-luciferase reporter assay system (Promega). The level of luciferase activity was calculated as a TOPFlash/FOPFlash reporter ratio excluding the effect of the minimal promoter activity. *Renilla* luciferase was used as a normalizer. The luciferase activity of the empty vector was set to 1. Results are presented as the mean ± SEM of at least three independent experiments performed in triplicate.

RESULTS

Identification of candidate biallelic *WNT7B* variants

- **Family 1:** We studied a female fetus who displayed a phenotype consistent with PDAC syndrome but without any pathogenic variant in *STRA6* or *RARB* (Fig. 1A, Table S2, P1). Briefly, the pregnancy was terminated at 35 6/7 weeks of gestation because of the presence of several abnormalities on the obstetrical ultrasound, including polyhydramnios, bilateral microphthalmia, retrognathia, atrial septal defect, poor cortico-medullary differentiation of the kidneys and a large bladder. Nuchal translucency was 1mm at 12 weeks of gestation. The fetus weighed 2060 grams (10th centile). The autopsy revealed multiple major abnormalities, including microphthalmia with dysplastic retina (Fig. 2), choanal atresia, agenesis of the larynx and trachea, bilateral pulmonary agenesis, atrial septal defect, diaphragmatic eventration, and hypoplastic kidneys (combined weight: 10.3 grams; reference values: 20 +/- 4 grams) with pyelocalyceal dilatation and medullary cysts involving distal and collecting tubules (Fig. 2). Dysmorphic features including tall forehead, frontal hirsutism, large anterior fontanel, small palpebral fissures, flat nasal bridge, microretrognathia. Neuropathological examination did not reveal any gross nor microscopic brain abnormalities. The parents were first cousins and originated from Tunisia.

Because of the parental consanguinity in this family, we analyzed the ES dataset of the affected fetus for rare homozygous variants. We identified 11 variants meeting these criteria (Table S3). Because of the presence of microphthalmia, we next focused our attention on variants in genes associated with eye development. By using the integrated Systems Tool for Eye gene discovery (iSyTE), we found that 2 of these variants (p.(Arg98*) in *WNT7B* and p.(Arg1281Lys) in *TRIOBP*) were expressed during eye development. *TRIOBP* pathogenic variants have previously been

associated with autosomal recessive deafness⁷, and thus, the highest priority variant was the homozygous nonsense variant in *WNT7B* (c.292C>T, p.(Arg98*)). Consistent with a recessive mode of inheritance, the c.292C>T variant in *WNT7B* was further confirmed by Sanger sequencing to be homozygous in the proband and heterozygous in the parents (Fig. 1A).

The *WNT7B* gene includes 4 exons, which encode a 349 amino-acid growth factor that comprises N- and C-terminal domains connected by a linker (Fig 1B). The c.292C>T variant in *WNT7B* is absent from public SNP databases (1000 Genomes, EVS, dbSNP138, GnomAD) and from CHU Sainte-Justine Research Center exome dataset (n>1000). It is located in the second exon, which is present in all 5 known *WNT7B* isoforms. The c.292C>T variant is likely inducing a loss of WNT7B function as it is predicted to abolish the C-terminal part of the protein encoded by exons 3 and 4, which binds to the Frizzled receptors (Fig. 1B).⁸ Indeed, deletion of exon 3 and 4 results in a null allele in mice.⁹ In addition, the c.292C>T variant may induce degradation of the transcript through the non-sense mediated mRNA decay system triggered upon the association of UPF1 with an Exon Junction Complex.¹⁰

We next used Sanger sequencing to search for rare variants in *WNT7B* in 17 additional individuals with features of the PDAC syndrome. This screen did not reveal any candidate variant in this gene. We then queried *WNT7B* in GeneMatcher, a freely accessible website that enables the identification of individuals with variants in candidate genes. We identified three matches for *WNT7B*, which correspond to the families described hereafter (Families 2, and 3):

- **Family 2** is non-consanguineous and from the UK. The proband, a female, was born at 37 weeks of gestation following a pregnancy with late polyhydramnios. She died quickly after birth (Fig 1A, Table S2, P21). Post mortem revealed a dysmorphic baby with a very broad nasal bridge, a high arched palate and a weight and head circumference within normal limits. Internally there

were major abnormalities of the respiratory and cardiovascular systems with marked pulmonary hypoplasia (combined lung weight = 3.66 g, 10% of that expected), tracheomalacia affecting much of the trachea, and a small proximal trachea-oesophageal fistula. Histology of the left lung showed primarily bronchial structures although the right lung was more appropriate for gestational age. There was total anomalous pulmonary venous drainage (TAPVD) with an absent right pulmonary vein, a small left pulmonary vein of uncertain course, an absent right pulmonary artery and extremely small left pulmonary artery. There was also a large secundum atrial septum defect and the diaphragms appeared elevated although they were not deficient. Kidneys were hypoplastic with scattered sclerosed glomeruli. The eyes were not examined. Brain displays severe autolysis but no specific abnormalities was identified and prenatal ultrasound scans did not reveal any cerebral anomaly.

The second pregnancy was interrupted at 24 weeks of gestation after ultrasound scan evidenced severe lung hypoplasia with highly placed diaphragms and the heart at the apex of the chest. This fetus (Table S2, P22) displayed retromicrognathia as well as heart and lung anomalies similar to those found in P21, including lung hypoplasia (combined pulmonary weight <10% of that expected), total anomalous pulmonary venous drainage, no pulmonary veins attached to the heart and normal pulmonary arteries. No tracheal abnormality was noted. Kidneys were structurally normal but hypoplastic (weighing 3.26 g combined versus 6.5 +/- 2.1 g expected). The eyes showed bilateral microphthalmia (axial length of 9.5 mm) with posterior inferior colobomas in both eyes and a dysplastic retina in the right eye (Fig 3). There was no brain significant abnormality.

WES in the first affected patient (P21) in Family 2 revealed the presence of compound heterozygous variants in *WNT7B* (c.225C>G, p.(Tyr75*) and c.562G>A, p.(Gly188Ser)). Both variants were found by Sanger sequencing in the second affected patient of this family (P22), and

both parents were found to each harbour one of the two identified variants (Fig 1A). The nonsense p.(Tyr75*) is absent from public databases (1000 Genomes, EVS, dbSNP138, GnomAD) and is located in the second exon, as it was also the case for p.(Arg98Ter), found in Family 1. The c.562G>A (p.(Gly188Ser)) is present heterozygous only once among 232162 alleles in GnomAD, and is predicted damaging by several *in silico* tools (*SIFT* [score: 0], *MutationTaster* [p-value:1], *Polyphen-2* [HumDiv score: 1; HumVar score: 0.99] and CADD [score:26]). The involved amino acid belongs to a stretch of residues that are conserved in mammals, chicken and zebrafish (Fig 1C).

- **Family 3**, a healthy consanguineous couple from Tunisia gave birth to two newborn babies who died immediately after birth (at 37 and 39 weeks of gestation, respectively) from respiratory distress and edema (Table S2, P23 and P24). Prenatal ultrasound scans did not reveal any cerebral anomaly.

We have little information regarding these newborns. However, severe lung hypoplasia was documented in both newborns and parietal skull bone softening was observed in one of them. Since the DNA was unavailable from either demised babies, we resorted to a molecular autopsy by proxy approach using ES¹¹, which revealed that both parents were heterozygous for the p.(Arg98*) variant (Fig 1A). Interestingly, this nonsense variant was also found in Family 1.

The three identified *WNT7B* variants (c.225C>G, c.292C>T, and c.562G>A) could be classified as pathogenic (class 5) based on the ACMG criteria (Table S4).

Functional validation of candidate variants

In order to demonstrate the deleterious effects of the identified variants on protein function, we conducted *in vitro* functional studies. We studied the functional impact of the variants on the

WNT- β -Catenin signaling pathway using a dual luciferase reporter assay. All three WNT7B variants, p.(Tyr75Ter), p.(Arg98Ter), and p.(Gly188Ser) showed reduced WNT7B signalling compared to the wild-type control ($P < 0.001$), consistent with the proposed deleterious effect of the identified variants (Fig 4). The p.(Arg98Ter) variant WNT7B signaling was lower compared with the p.(Tyr75Ter) variant ($P = 0.012$) and the p.(Gly188Ser) variant ($P < 0.001$), perhaps reflecting more marked instability of the p.Arg89Ter peptide. *In vivo*, both nonsense variants would be expected to be subjected to nonsense mediated decay, which is not modelled in this assay which uses intronless expression clones. This luciferase assay demonstrates that any transcripts that may escape nonsense mediated decay would not result in functional protein.

Zebrafish mutant lines analysis

We next sought to assess the impact of a loss of *wnt7ba* and/or *wnt7bb* on the morphology of adult zebrafish. Compared with wild-type fish, *wnt7ba*^{-/-} and *wnt7bb*^{-/-} mutants showed no gross morphological anomalies of the eye, heart and kidney (Fig 5a). However, we observed that the swimbladder of the *wnt7bb*^{-/-} mutant was formed by a single chamber contrary to the presence of anterior and posterior chambers in the wild-type and *wnt7ba*^{-/-} counterparts (Fig. 5b). No difference of viability was observed between the wild-type, *wnt7ba*^{+/-}, *wnt7bb*^{+/-}, *wnt7ba*^{-/-}, *wnt7bb*^{-/-} as well as double heterozygous (*wnt7ba*^{+/-};*wnt7bb*^{+/-}) fish. In contrast, the genotyping of 500 fish from *wnt7ba*^{+/-} x *wnt7bb*^{+/-} mating showed the absence of the *wnt7ba*^{-/-};*wnt7bb*^{-/-} genotype at two months of age, suggesting that these two genes have redundant functions for development and/or survival in the zebrafish.

DISCUSSION

We identified rare and likely deleterious biallelic variants in *WNT7B* in 3 patients with severe lung hypoplasia from two unrelated families. These patients showed a pattern of malformations, including microphthalmia, lung hypoplasia and cardiac defects, that is similar to the PDAC syndrome. Interestingly, we also identified two siblings from a third family (Family 3) whose parents were carrying the same nonsense variant in *WNT7B* as in Family 1. Although phenotyping of these siblings was limited, both showed severe lung hypoplasia. It thus appears likely that these siblings were homozygous for the nonsense variant, further supporting the association between *WNT7B* disruption and lung hypoplasia. The fact that such variants were independently found in multiple unrelated families with a similar pattern of malformations strongly suggests a causal link.

WNT7B belongs to a large family of growth factors that regulate diverse aspects of embryonic development by binding to specific receptors on the cell surface.¹² In different tissues, *WNT7B* functions via distinct signaling pathways, including the canonical β -catenin pathway^{9 13}, the non-canonical planar cell polarity pathway¹⁴ and the G-protein-linked PKC delta pathway¹⁵. In the WNT- β -catenin pathway, *WNT7B* binds to a Frizzled receptor and to one of the low-density lipoprotein-related receptor 5 or 6 (LRP5/6), which leads to the stabilization of the transcriptional activator β -catenin and activation of target genes. Mice with a loss of *Wnt7b* function die at embryonic day 9.5, before the onset of organogenesis, as *Wnt7b* is essential for placental development.⁹ Mice homozygous for hypomorphic mutations or for a conditional null mutation induced in cells of the epiblast survive until birth but show severe lung hypoplasia.^{16 17} *WNT7B* appears to regulate lung development via the canonical WNT- β -catenin pathway by reducing

proliferation in both the epithelium and mesenchyme.^{17 18} The presence of a similar phenotype of lung hypoplasia in our cases provides some support for the pathogenic involvement of *WNT7B*.

The swimbladder is an air-filled organ that is a structural homolog of the mammalian lung¹⁹ and a suite of genes, including *Wnt7b*, *Nkx2.1*, *FoxA2*, and *Gata6*, have been shown to be co-expressed during the development of the swimbladder in the zebrafish and of the lung in mice.^{17,20} We found that the knock-out of *wnt7bb*, but not of *wnt7ba*, disrupts the development of the swimbladder, suggesting that WNT7B function has been conserved through evolution, being required for the proper development of the swimbladder in fish and of the lung in mammals. We also found that *wnt7ba* and *wnt7bb* functions were redundant in the zebrafish. Detailed characterization of double mutants will be necessary to fully understand the function of these genes in this model.

Not only is WNT7B required for the development of the lung in mice but it also plays a role in the development of the trachea, eyes and kidneys, all of which are affected in at least some of our patients. For instance, the fetus from Family 1 showed agenesis of the larynx and trachea, and one fetus from Family 2 had tracheal and bronchi cartilage abnormalities. The trachea of mice with a conditional null allele of *Wnt7b* appears normal in length and diameter but their cartilaginous rings are incomplete.¹⁷ There is additional evidence from organotypic culture studies that canonical WNT signaling is required for tracheal chondrogenesis.²¹

WNT7/β-catenin signaling has also been demonstrated to be essential for eye development by controlling morphogenesis of the optic cup and patterning of the ocular tissue, promoting the differentiation of the retinal pigment epithelium, and maintaining the dorsal retinal identity.²² *Wnt7b* is strongly expressed in the developing retina and lens in mice.^{23 24} Interestingly, expression of *Wnt7b* in the developing brain of the mouse has been shown to be regulated by *Pax6*, which is

1
2
3 implicated in the pathogenesis of microphthalmia and anophthalmia.²⁵ Studies performed in mice
4
5 with a hypomorphic variant in *Wnt7b* showed that macrophage WNT7B is a short-range paracrine
6
7 signal required for programmed cell death in the vascular endothelial cells of the temporary hyaloid
8
9 vessels of the post-natal eye.¹³ Moreover, *WNT7B* variants have previously been associated with
10
11 myopia and central corneal thickness.^{26,27} Our work indicates that WNT7B is also required at earlier
12
13 stages of eye development. Additional studies in animal models will be necessary to dissect this
14
15 role at the molecular and cellular levels.
16
17

18
19 *Wnt7b* also functions in the developing kidney where it is expressed in the future collecting
20
21 duct network.²⁸ In *Wnt7b* conditional null mice, the cortical epithelial development is normal but
22
23 the medullary zone fails to develop properly, being characterized by the presence of dilated
24
25 collecting tubules and the poor growth of the loops of Henle.²⁸ The kidneys of the 3 fetuses in
26
27 Family 1 and 2 were hypoplastic. In addition, the kidneys of the fetus from Family 1 were
28
29 characterized by the presence of medullary cysts involving distal and collecting tubules dilatation
30
31 without any involvement of the cortical domain. Overall, these observations suggest that the
32
33 function of WNT7B in the developing kidney has been conserved in humans.
34
35
36

37
38 *WNT7B* belongs to a family of 19 genes that play critical roles for the development of
39
40 multiple organs and systems. Less than half of these genes have been associated with rare human
41
42 disorders, mainly developmental defects affecting the bones, teeth, and skin.¹² By involving
43
44 *WNT7B* in the pathogenesis of PDAC syndrome, our study thus broadens the spectrum of human
45
46 developmental disorders caused by disruption of *WNT* genes.
47
48

49
50 Pathogenic variants in *STRA6* and *RARB* have previously been shown to cause PDAC
51
52 syndrome.^{2,3} Indeed, the phenotypes associated with the disruption of *STRA6*, *RARB* and *WNT7B*
53
54 are similar, with the involvement of the lungs and kidneys being more frequent in patients with
55
56
57
58
59
60

1
2
3 variants in *STRA6* and *WNT7B* than in those with variants in *RARB* (Table S5). Both *STRA6* and
4
5 *RARB* are implicated in retinoic acid signaling. Interestingly, some studies indicate that lung
6
7 hypoplasia associated with retinoic acid deficiency is mediated at least in part by the disruption of
8
9 WNT signalling.²⁹ All together, these observations thus raise the possibility that some of the
10
11 features of PDAC syndrome involve developmental processes that are regulated by an interaction
12
13 between the retinoic acid and WNT pathways. Further studies, however, will be needed to confirm
14
15 a functional link between *STRA6*, *RARB* and *WNT7B*.
16
17
18
19
20
21
22
23
24
25
26
27
28
29
30
31
32
33
34
35
36
37
38
39
40
41
42
43
44
45
46
47
48
49
50
51
52
53
54
55
56
57
58
59
60

Funding

This work was supported by grants from the Fondation Jeanne et Jean-Louis Lévesque (JLM), Fondation Maladies Rares (NC), Retina France (NC, LFT), NHMRC Grant 1099165 (RVJ) and Costco and Luminesce Alliance (LGR). We acknowledge Nicolas Fossat for assistance with vector cloning. We thank the Sequencing and Genotyping Core Facilities at KFSHRC for their technical help. The authors extend their appreciation to the King Salman Center For Disability Research for funding this work through Research Group no RG-2022-011. French patients were recruited through the Rares Diseases Cohorts (RaDiCo) program which is funded by the French National Research Agency under the specific program “Investments for the Future”, Cohort grant agreement ANR-10-COHO-0003.

Competing interests

None

Ethics approval statement

Research has been performed in accordance with the Declaration of Helsinki. This study was approved by the CHU Sainte-Justine, by the Sud-Ouest and Outre-Mer II and by the King Faisal Specialist Hospital (KFSRHC RAC#2070023) ethics research boards. Informed consent was obtained from all participants or their legal guardians.

Contributorship Statement

FSA, JLM, RJ and NC contributed to the study conception and design. Patients recruitment and clinical evaluations were performed by NAA, JB, MAA, JM, SH, HSL, TAB, PC and NC. WES

1
2
3 were performed and analysed by FH, CN, NP and FSA. Sanger sequencing were performed by SJ,
4
5 PC, and NC. Zebrafish studies were performed by SBou, SBoi, LFT, JMR, MM, CN, MD, and SE.
6
7 *In vitro* analyses were performed by LGR, RG, DW, IP, and RJ. The first draft of the manuscript
8
9 was written by SBou, JLM and NC and all authors commented on previous versions of the
10
11 manuscript. All authors read and approved the final manuscript.
12
13
14
15
16

17 **Acknowledgments**

18
19 We acknowledge the generous support from the families published in this article.
20
21
22
23
24
25
26
27
28
29
30
31
32
33
34
35
36
37
38
39
40
41
42
43
44
45
46
47
48
49
50
51
52
53
54
55
56
57
58
59
60

Supplemental Data

Supplemental Data include five tables.

Accession numbers

The ClinVar (<https://www.ncbi.nlm.nih.gov/clinvar/>) accession numbers for the variants reported in this article are: SCV001976485 (c.225C>G); SCV000598632 (c.292C>T); SCV001976486 (c.562G>A).

References

1. Meller CH, Morris RK, Desai T, Kilby MD. Prenatal diagnosis of isolated right pulmonary agenesis using sonography alone: case study and systematic literature review. *J Ultrasound Med* 2012;31(12):2017-23
2. Pasutto F, Sticht H, Hammersen G, Gillessen-Kaesbach G, Fitzpatrick DR, Nurnberg G, Brasch F, Schirmer-Zimmermann H, Tolmie JL, Chitayat D, Houge G, Fernandez-Martinez L, Keating S, Mortier G, Hennekam RC, von der Wense A, Slavotinek A, Meinecke P, Bitoun P, Becker C, Nurnberg P, Reis A, Rauch A. Mutations in STRA6 cause a broad spectrum of malformations including anophthalmia, congenital heart defects, diaphragmatic hernia, alveolar capillary dysplasia, lung hypoplasia, and mental retardation. *Am J Hum Genet* 2007;80(3):550-60
3. Srour M, Chitayat D, Caron V, Chassaing N, Bitoun P, Patry L, Cordier MP, Capo-Chichi JM, Francannet C, Calvas P, Ragge N, Dobrzyniecka S, Hamdan FF, Rouleau GA, Tremblay A, Michaud JL. Recessive and dominant mutations in retinoic acid receptor beta in cases with microphthalmia and diaphragmatic hernia. *Am J Hum Genet* 2013;93(4):765-72
4. Sobreira N, Schiettecatte F, Valle D, Hamosh A. GeneMatcher: a matching tool for connecting investigators with an interest in the same gene. *Hum Mutat* 2015;36(10):928-30
5. Beretta CA, Brinkmann I, Carl M. All four zebrafish Wnt7 genes are expressed during early brain development. *Gene Expr Patterns* 2011;11(3-4):277-84
6. Wang Z, Shu W, Lu MM, Morrissey EE. Wnt7b activates canonical signaling in epithelial and vascular smooth muscle cells through interactions with Fzd1, Fzd10, and LRP5. *Mol Cell Biol* 2005;25(12):5022-30
7. Shahin H, Walsh T, Sobe T, Abu Sa'ed J, Abu Rayan A, Lynch ED, Lee MK, Avraham KB, King MC, Kanaan M. Mutations in a novel isoform of TRIOBP that encodes a filamentous-actin binding protein are responsible for DFNB28 recessive nonsyndromic hearing loss. *Am J Hum Genet* 2006;78(1):144-52
8. Janda CY, Waghray D, Levin AM, Thomas C, Garcia KC. Structural basis of Wnt recognition by Frizzled. *Science* 2012;337(6090):59-64
9. Parr BA, Cornish VA, Cybulsky MI, McMahon AP. Wnt7b regulates placental development in mice. *Dev Biol* 2001;237(2):324-32
10. Kurosaki T, Maquat LE. Nonsense-mediated mRNA decay in humans at a glance. *J Cell Sci* 2016;129(3):461-7
11. Shamseldin HE, Kurdi W, Almusafri F, Alnemer M, Alkaff A, Babay Z, Alhashem A, Tulbah M, Alsahan N, Khan R, Sallout B, Al Mardawi E, Seidahmed MZ, Meriki N, Alsaber Y, Qari A, Khalifa O, Eyaid W, Rahbeeni Z, Kurdi A, Hashem M, Alshidi T, Al-Obeid E, Abdulwahab F, Ibrahim N, Ewida N, El-Akouri K, Al Mulla M, Ben-Omran T, Pergande M, Cirak S, Al Tala S, Shaheen R, Fageih E, Alkuraya FS. Molecular autopsy in maternal-fetal medicine. *Genet Med* 2018;20(4):420-27
12. Nusse R, Clevers H. Wnt/beta-Catenin Signaling, Disease, and Emerging Therapeutic Modalities. *Cell* 2017;169(6):985-99
13. Lobov IB, Rao S, Carroll TJ, Vallance JE, Ito M, Ondr JK, Kurup S, Glass DA, Patel MS, Shu W, Morrissey EE, McMahon AP, Karsenty G, Lang RA. WNT7b mediates macrophage-induced programmed cell death in patterning of the vasculature. *Nature* 2005;437(7057):417-21
14. Rosso SB, Sussman D, Wynshaw-Boris A, Salinas PC. Wnt signaling through Dishevelled, Rac and JNK regulates dendritic development. *Nat Neurosci* 2005;8(1):34-42

15. Tu X, Joeng KS, Nakayama KI, Nakayama K, Rajagopal J, Carroll TJ, McMahon AP, Long F. Noncanonical Wnt signaling through G protein-linked PKCdelta activation promotes bone formation. *Dev Cell* 2007;12(1):113-27

16. Shu W, Jiang YQ, Lu MM, Morrissey EE. Wnt7b regulates mesenchymal proliferation and vascular development in the lung. *Development* 2002;129(20):4831-42

17. Rajagopal J, Carroll TJ, Guseh JS, Bores SA, Blank LJ, Anderson WJ, Yu J, Zhou Q, McMahon AP, Melton DA. Wnt7b stimulates embryonic lung growth by coordinately increasing the replication of epithelium and mesenchyme. *Development* 2008;135(9):1625-34

18. Aros CJ, Pantoja CJ, Gomperts BN. Wnt signaling in lung development, regeneration, and disease progression. *Commun Biol* 2021;4(1):601

19. Torday JS, Rehan VK. Deconvoluting lung evolution using functional/comparative genomics. *Am J Respir Cell Mol Biol* 2004;31(1):8-12

20. Cass AN, Servetnick MD, McCune AR. Expression of a lung developmental cassette in the adult and developing zebrafish swimbladder. *Evol Dev* 2013;15(2):119-32

21. Snowball J, Ambalavanan M, Whitsett J, Sinner D. Endodermal Wnt signaling is required for tracheal cartilage formation. *Dev Biol* 2015;405(1):56-70

22. Fujimura N. WNT/beta-Catenin Signaling in Vertebrate Eye Development. *Front Cell Dev Biol* 2016;4:138

23. Liu H, Mohamed O, Dufort D, Wallace VA. Characterization of Wnt signaling components and activation of the Wnt canonical pathway in the murine retina. *Dev Dyn* 2003;227(3):323-34

24. Ang SJ, Stump RJ, Lovicu FJ, McAvoy JW. Spatial and temporal expression of Wnt and Dickkopf genes during murine lens development. *Gene Expr Patterns* 2004;4(3):289-95

25. Williamson KA, FitzPatrick DR. The genetic architecture of microphthalmia, anophthalmia and coloboma. *Eur J Med Genet* 2014;57(8):369-80

26. Gao X, Nannini DR, Corrao K, Torres M, Chen YI, Fan BJ, Wiggs JL, International Glaucoma Genetics C, Taylor KD, Gauderman WJ, Rotter JI, Varma R. Genome-wide association study identifies WNT7B as a novel locus for central corneal thickness in Latinos. *Hum Mol Genet* 2016;25(22):5035-45

27. Miyake M, Yamashiro K, Tabara Y, Suda K, Morooka S, Nakanishi H, Khor CC, Chen P, Qiao F, Nakata I, Akagi-Kurashige Y, Gotoh N, Tsujikawa A, Meguro A, Kusuhara S, Polasek O, Hayward C, Wright AF, Campbell H, Richardson AJ, Schache M, Takeuchi M, Mackey DA, Hewitt AW, Cuellar G, Shi Y, Huang L, Yang Z, Leung KH, Kao PYP, Yap MKH, Yip SP, Moriyama M, Ohno-Matsui K, Mizuki N, MacGregor S, Vitart V, Aung T, Saw SM, Tai ES, Wong TY, Cheng CY, Baird PN, Yamada R, Matsuda F, Nagahama Study G, Yoshimura N. Identification of myopia-associated WNT7B polymorphisms provides insights into the mechanism underlying the development of myopia. *Nat Commun* 2015;6:6689

28. Yu J, Carroll TJ, Rajagopal J, Kobayashi A, Ren Q, McMahon AP. A Wnt7b-dependent pathway regulates the orientation of epithelial cell division and establishes the cortico-medullary axis of the mammalian kidney. *Development* 2009;136(1):161-71

29. Chen F, Cao Y, Qian J, Shao F, Niederreither K, Cardoso WV. A retinoic acid-dependent network in the foregut controls formation of the mouse lung primordium. *J Clin Invest* 2010;120(6):2040-8

Figure Legends

Figure 1. *WNT7B* variants identified in this study. (A) Pedigrees of the three families showing segregation of the variants in *WNT7B*. (B) Localization of the variants with respect to the primary structure of *WNT7B*. This protein comprises two structural domains, a large N-terminal (NTD) and a C-terminal domain (CTD), which are connected by a linker sequence. (C) Conservation of the Gly188 residue across various species.

Figure 2. Histology and immunohistochemical analysis of the eyes and kidneys of patient 1. (A,B) Eye histology. (A) Left eye (H&E, x0,5): Microphthalmia with global retinal detachment. (B) Right eye (H&E, x0,5): Microphthalmia with retinal rings ("rosettes") at the level of optic nerve insertion. (C-H) Renal histology. (C) Right kidney (H&E, x0,5): Cortico-medullary differentiation is preserved in all reniculi, although the renal parenchyma is compressed by pyelo-caliceal dilatation. (D) Right kidney (H&E, x2): Number of medullary cysts surrounded by the immature mesenchymal rings. (E): Right kidney (EMA, x0,5): Right kidney showing the diffuse positivity as expected in distal and collecting tubes. (F) Right kidney (EMA, x2): Note positive staining on all medullary cysts. (G): Right kidney (CD10, x0,5): Right kidney showing the diffuse positivity as expected in glomeruli and proximal tubules. (H) Right kidney (CD10, x2): Negative staining on microcysts in medulla.

Figure 3. Histology analysis of the eyes of patient 22. (A) H&E (Haematoxylin and eosin) stained section of the right globe. L=lens; R=retina; S=sclera. The arrow points to a gap in the sclera that indicates the posterior coloboma, through which retina is prolapsing. (B) H&E stained section of the right globe. L=lens; R=retina; S=sclera; ON=optic nerve. This section is parasagittal to the scleral coloboma defect in plate A with the arrow pointing to colobomatous extraocular retinal tissue adjacent to the optic nerve. (C) H&E of the intraocular retina, showing the dysplastic rosettes (arrows). (D) H&E higher power of the colobomatous extraocular retinal tissue adjacent to the optic nerve, showing retinal neuronal cell bodies on the left and the looser eosinophilic glial tissue to the right.

Figure 4. Impact of the *WNT7B* variants on *WNT7B* signalling in a dual luciferase reporter assay. HEK293T cells were co-transfected with pCMVSPORT6/*WNT7B* (WT or variant), LRP5, TOPFlash/FOPFlash plasmids, and *Renilla* plasmid. *WNT7B* signalling was measured 24 h later by a dual luciferase reporter assay. Experiments were done at least 3 times in triplicate and results are expressed as means \pm S.E.M. Asterisks above bars indicate results from a Student's t-test for *WNT7B* variants or the empty pCMV-SPORT6 vector compared to WT *WNT7B* (***) $p < 0.001$). All three variants demonstrated reduced *WNT7B* signalling compared with the wild-type control.

Figure 5. Histological and X-ray analysis of adults zebrafish. (A) Sections of WT and mutants (*wnt7ba*^{-/-} / *wnt7bb*^{-/-}) zebrafish adult kidneys, hearts and eyes (7-9 months old) were stained with PAS and H&E. Homozygous mutants did not appear to have major abnormalities in kidneys, heart and eyes morphology. (B) X-rays reveal severe anomalies of the swimbladder (absence of the posterior chamber indicated by a star) in the *wnt7bb*^{-/-} mutant (n=10) but not in the *wnt7ba*^{-/-} paralog. Abbreviations: CD (Collecting duct) ; G (Glomerulus) ; PT (Proximal tubules) ; DT (Distal tubule) ; V (Ventricle) ; BA (Bulbus arteriosus) ; A (Atrium) ; R (Retina) ; L (Lens) ; C (Cornea) ; I (Iris).

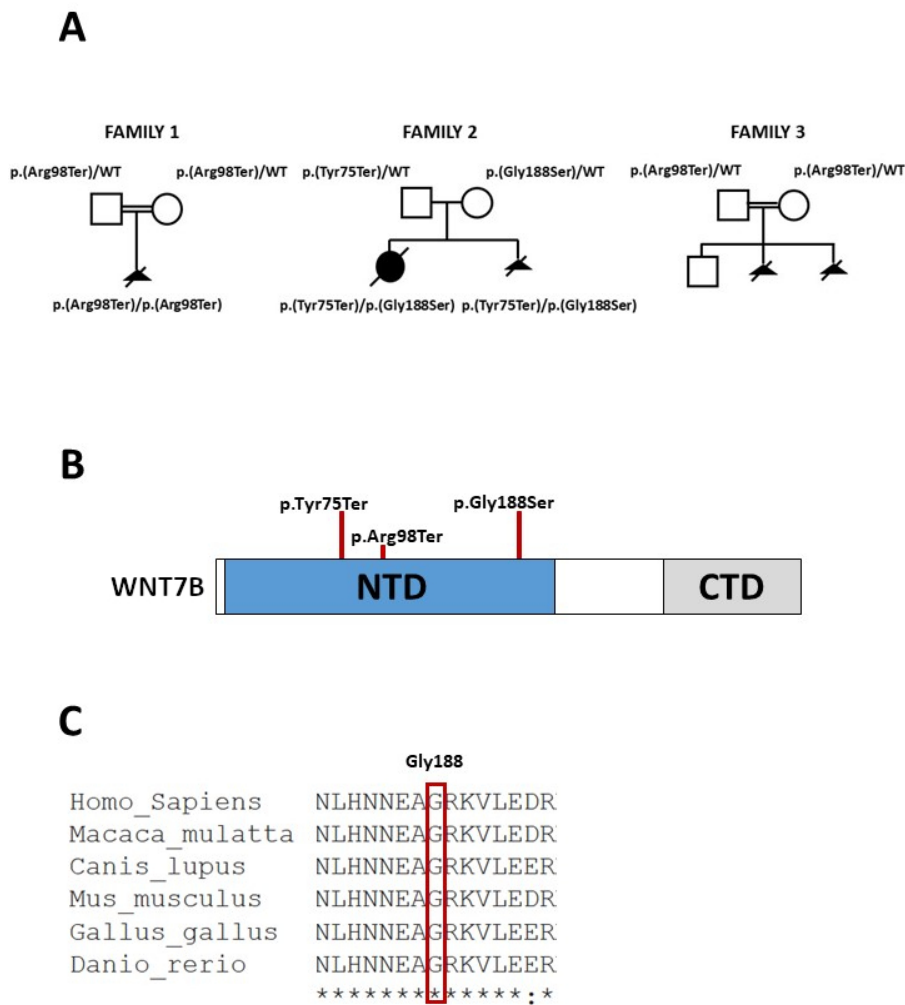


Figure 1. WNT7B variants identified in this study. (A) Pedigrees of the three families showing segregation of the variants in WNT7B. (B) Localization of the variants with respect to the primary structure of WNT7B. This protein comprises two structural domains, a large N-terminal (NTD) and a C-terminal domain (CTD), which are connected by a linker sequence. (C) Conservation of the Gly188 residue across various species.

60x81mm (300 x 300 DPI)

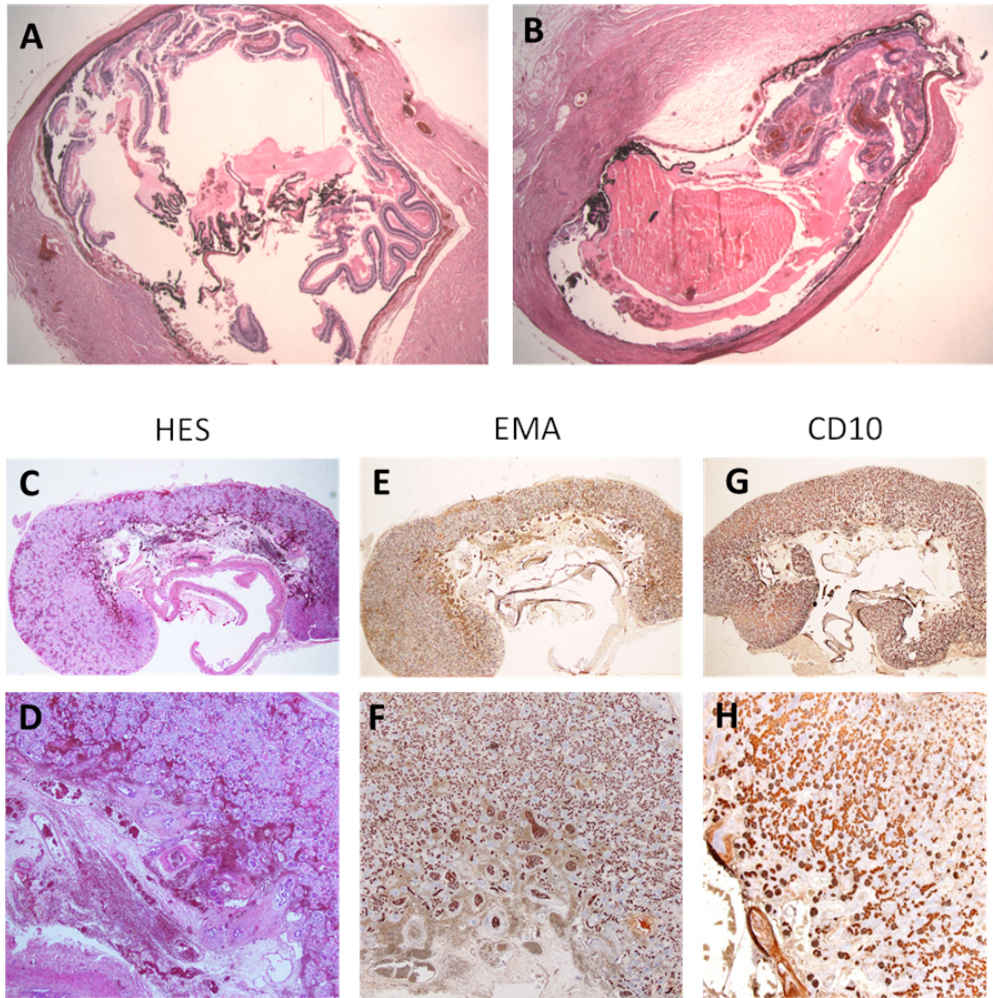


Figure 2. Histology and immunohistochemical analysis of the eyes and kidneys of patient 1. (A,B) Eye histology. (A) Left eye (H&E, x0,5): Microphthalmia with global retinal detachment. (B) Right eye (H&E, x0,5): Microphthalmia with retinal rings ("rosettes") at the level of optic nerve insertion. (C-H) Renal histology. (C) Right kidney (H&E, x0,5): Cortico-medullar differentiation is preserved in all renicules, although the renal parenchyma is compressed by pyelo-caliceal dilatation. (D) Right kidney (H&E, x2): Number of medullary cysts surrounded by the immature mesenchymal rings. (E): Right kidney (EMA, x0,5): Right kidney showing the diffuse positivity as expected in distal and collecting tubes. (F) Right kidney (EMA, x2): Note positive staining on all medullary cysts. (G): Right kidney (CD10, x0,5): Right kidney showing the diffuse positivity as expected in glomeruli and proximal tubules. (H) Right kidney (CD10, x2): Negative staining on microcysts in medulla.

76x76mm (300 x 300 DPI)

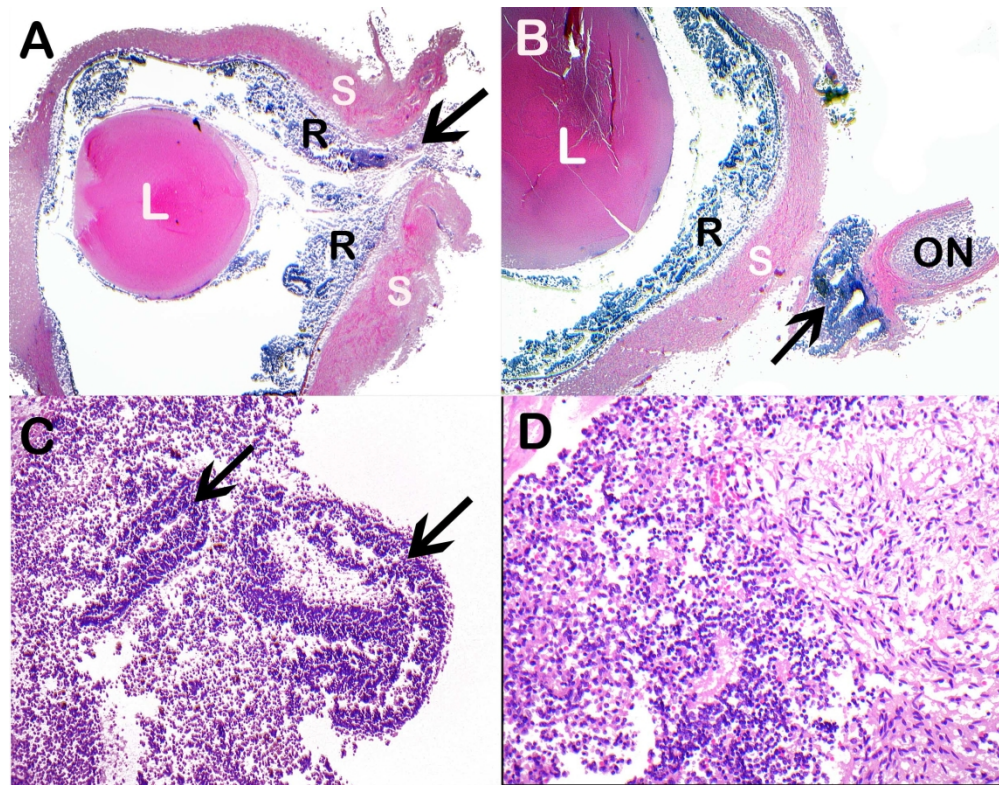


Figure 3. Histology analysis of the eyes of patient 22. (A) H&E (Haematoxylin and eosin) stained section of the right globe. L=lens; R=retina; S=sclera. The arrow points to a gap in the sclera that indicates the posterior coloboma, through which retina is prolapsing. (B) H&E stained section of the right globe. L=lens; R=retina; S=sclera; ON=optic nerve. This section is parasagittal to the scleral coloboma defect in plate A with the arrow pointing to colobomatous extraocular retinal tissue adjacent to the optic nerve. (C) H&E of the intraocular retina, showing the dysplastic rosettes (arrows). (D) H&E higher power of the colobomatous extraocular retinal tissue adjacent to the optic nerve, showing retinal neuronal cell bodies on the left and the looser eosinophilic glial tissue to the right.

209x163mm (300 x 300 DPI)

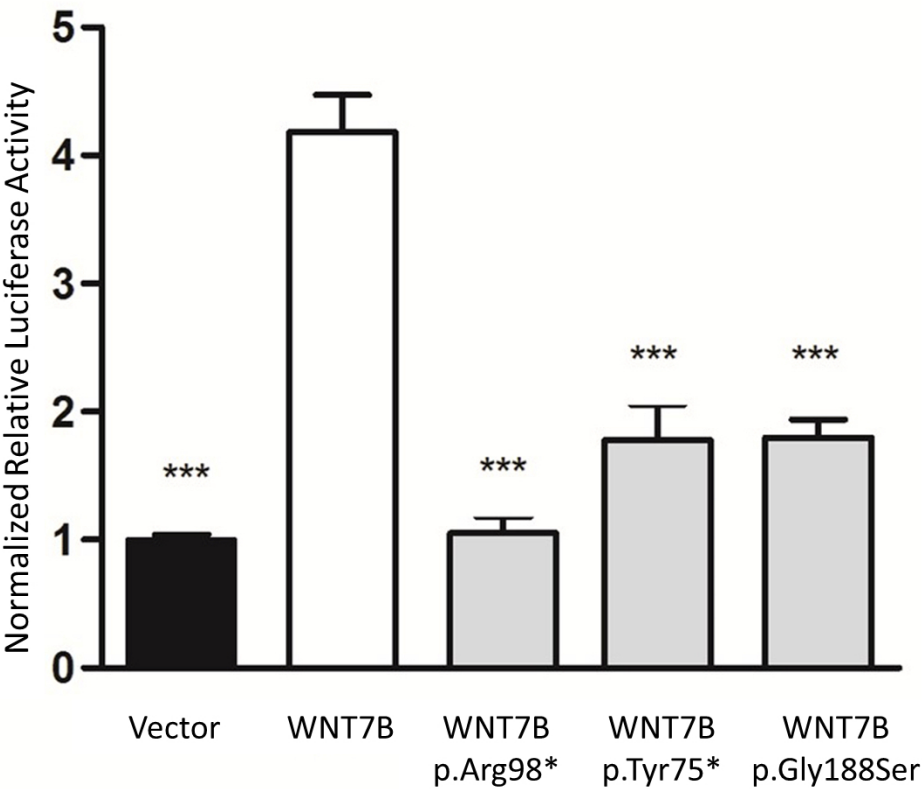


Figure 4. Impact of the WNT7B variants on WNT7B signalling in a dual luciferase reporter assay. HEK293T cells were co-transfected with pCMVSPORT6/WNT7B (WT or variant), LRP5, TOPFlash/FOPFlash plasmids, and Renilla plasmid. WNT7B signalling was measured 24 h later by a dual luciferase reporter assay. Experiments were done at least 3 times in triplicate and results are expressed as means \pm S.E.M. Asterisks above bars indicate results from a Student's t-test for WNT7B variants or the empty pCMV-SPORT6 vector compared to WT WNT7B (*** $p < 0.001$). All three variants demonstrated reduced WNT7B signalling compared with the wild-type control.

96x86mm (300 x 300 DPI)

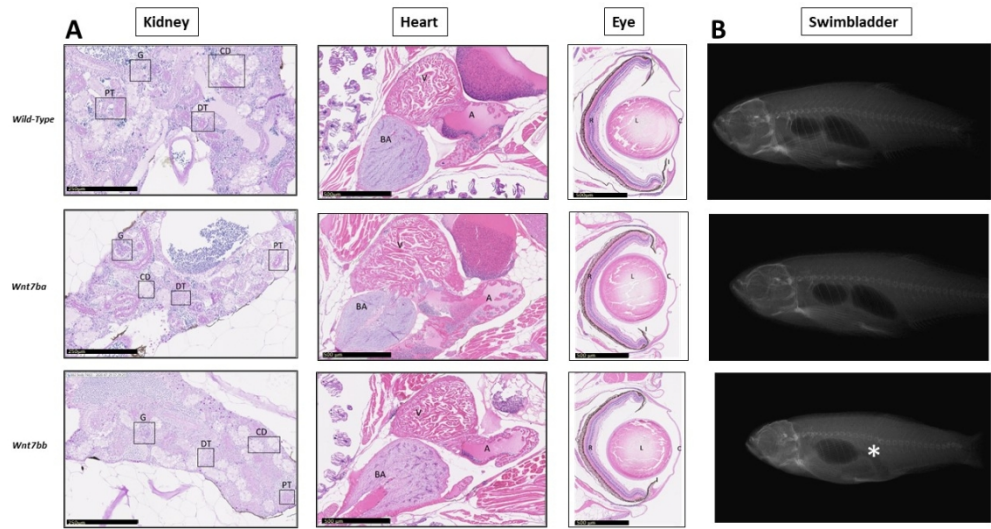


Figure 5. Histological and X-ray analysis of adults zebrafish. (A) Sections of WT and mutants (*wnt7ba*^{-/-} / *wnt7bb*^{-/-}) zebrafish adult kidneys, hearts and eyes (7-9 months old) were stained with PAS and H&E. Homozygous mutants did not appear to have major abnormalities in kidneys, heart and eyes morphology. (B) X-rays reveal severe anomalies of the swimbladder (absence of the posterior chamber indicated by a star) in the *wnt7bb*^{-/-} mutant (n=10) but not in the *wnt7ba*^{-/-} paralog. Abbreviations: CD (Collecting duct) ; G (Glomerulus) ; PT (Proximal tubules) ; DT (Distal tubule) ; V (Ventricle) ; BA (Bulbus arteriosus) ; A (Atrium) ; R (Retina) ; L (Lens) ; C (Cornea) ; I (Iris).

108x60mm (300 x 300 DPI)

Supplementary Table S1: Primers used for *WNT7B* Sanger sequencing

PRIMERS	SEQUENCES	Length (bp)
WNT7B-exon1A-F	TCAACCGGGCTTCGAGGT	469
WNT7B-exon1A-R	GAGGGTCTGACACACGGG	
WNT7B-exon2-F	AGTTGATGGGAAACAGCCCC	519
WNT7B-exon2-R	AGGCAAAGAAATTGGCCCCC	
WNT7B-exon3-F	CCTACCATAGCCCTGAGAGATG	664
WNT7B-exon3-R	ACATCTCTGGATGGGGACAGC	
WNT7B-exon4A-F	CCTGAAGGGCTGTGAGAGT	891
WNT7B-exon4A-R	GCTTCTGCACCCGTCTATGT	
WNT7B-exon1B-F	GAGCCTGTTTCAGCCCCG	305
WNT7B-exon1B-R	CCAAGTGCTCCACCTCGG	
WNT7B-exon1C-F	AGAATCTGTCTCGGCTTCGC	517
WNT7B-exon1C-R	ACAAACACCCAGGGACACAG	
WNT7B-exon4B-F	TCCATCTCTTATATGGACACTCTCA	353
WNT7B-exon4B-R	TTTCCGCACAGGCACCC	

These primers were used to amplify exons from the different *WNT7B* isoforms (ENST00000339464.8; ENST00000409496.7; ENST00000410058.1; ENST00000410089.5; and ENST00000428540.1)

Supplementary Table S2: Phenotypes of patients included in this study

Patient ID	Gender	PDAC features				Other	Consanguinity	Family History	WNT7B mutation
		P	D	A	C				
Patients screened by whole-exome sequencing									
P1	M	Bilateral agenesis	Bilateral diaphragmatic eventration	Bilateral microphthalmia, retinal dysplasia	Atrial septal defect	Choanal atresia, arachnodactyly, tracheo-laryngeal agenesis, hypoplastic kidneys	Yes		p.(Arg98Ter) homozygous
P2	F	Unilobular and hypoplastic right lung, absent left lung	Right diaphragmatic hernia	Bilateral anophthalmia	Complex cardiovascular malformations	Hypoplastic kidneys	No	2 brother stillborn with multiple congenital anomalies	No
P3	M	No	Right diaphragmatic hernia	Bilateral microphthalmia, sclerocornea	Ventricular septal defect, persistent truncus arteriosus	Tracheal atresia, spleen hypoplasia, horseshoe kidneys, camptodactyly	No	Previous TOP for diaphragmatic hernia	No
Patients screened by Sanger sequencing									
P4	M	Hypoplasia left lung	No	Bilateral microphthalmia, retinal dysplasia	No	IUGR, arthrogryposis, splenomegaly	No		No
P5	M	Bilateral agenesis	Right diaphragmatic hernia	Unilateral Axenfeld-Rieger anomaly	Double outlet right ventricle, pulmonary arterial hypoplasia	Laryngeal atresia, polysplenism, ectopic right kidney, anal imperforation with rectal atresia	No	1 affected brother	No
P6	F	Bilateral hypoplasia	Thin diaphragmatic cupula	No	No		No		No
P7	F	Unilobular and dysplastic left lung	No	Microphthalmia	Yes	Renal cysts, semi-circular canals hypoplasia	No		No
P8	F	No	No	Microphthalmia	Ventricular septal defect	Schizencephaly, ureteral duplication, vertebral abnormalities	No		No
P9	M	No	Absent left diaphragmatic cupula	Bilateral microphthalmia	No	Coelosomia, vesical extrophy, kidney hypoplasia, angulation of right femur, anal ante-position, polysplenia, absent pancreas	No		No
P10	M	Alveolo capillary dysplasia	No	No	Ventricular septal defect	Pyelo-ureteral dilatation	No		No

P11	F	Left agenesis, right hypoplastic unilobar lung	Bilateral diaphragmatic cupula herniation	Right colobomatous microphthalmia	Ventricular septal defect, pulmonary artery agenesis	Cleft palate, unilateral agenesis of right semi-circular canals, oeso-tracheal fistula	No		No
P12	F	Bilateral agenesis	No	No	No		No	1 affected sib	No
P13	M	No	No	Bilateral anophthalmia	No	Panhypopituitarism, meningocele, right carotid artery agenesis	No	Previous TOP for Fallot tetralogy and bilobular lung	No
P14	M	Right agenesis	No	No	Agenesis of right pulmonary arteria	2 hemivertebraes	No		No
P15	F	Acinous dysplasia	No	No	No		No		No
P16	F	Unilateral hypoplasia	Unilateral hernia	Unilateral microphthalmia with retinal dysplasia and anterior chamber abnormalities	No		No		No
P17	M	Bilateral hypoplasia	No	No	No	Bilateral cryptorchism, spleen hypoplasia	No		No
P18	M	Bilateral agenesis	No	Bilateral microphthalmia	Absent pulmonary veins	Pyelocalyceal dilation, cystic kidneys	No		No
P19	M	Right hypoplasia, unilobar lungs	No	Bilateral anophthalmia	Complex cardiovascular malformations	Cleft lip and palate, esophageal atresia, polysplenia, hypoplastic kidney	No		No
P20	M	Bilateral agenesis	Right diaphragmatic hernia	Bilateral anophthalmia	Absence of pulmonary veins, pulmonary artery hypoplastic	Holoprosencephaly, Cleft lip and palate,	No		No
Patients retrieved by GeneMatcher									
P21	F	Bilateral severe lung hypoplasia	Bilateral diaphragmatic hernia	Not examined	Large atrial septum defect, total anomalous pulmonary venous drainage	Large abnormal trachea and main bronchi cartilage, small trachea-oesophageal fistula, hypoplastic kidneys with scattered sclerosed glomeruli	No	Sib of P22	p.(Tyr75Ter) p.(Gly188Ser)
P22	F	Bilateral severe lung hypoplasia	No	Bilateral colobomatous microphthalmia, dysplastic retina	Total anomalous pulmonary venous drainage	Hypoplastic kidneys	No	Sib of P21	p.(Tyr75Ter) p.(Gly188Ser)

P23	M	Bilateral severe lung hypoplasia	Not examined	Not examined	Not examined	Skull bone softening	Yes	<u>Sib of P24</u>	Both parents carrying the p.(Arg98Ter) variation
P24	M	Bilateral severe lung hypoplasia	Not examined	Not examined	Not examined		Yes	<u>Sib of P23</u>	Both parents carrying the p.(Arg98Ter) variation

M: Male; F: Female; TOP: termination of pregnancy; IUGR: intra-uterine growth retardation

Supplementary Table S3: Variants retains after filtering step used to analyse exome results from Patient 1.

Chr	Position	Gene symbol	Reference	cDNA change	Protein change	OMIM link	SIFT score	Polyphen-2 score (HumVar)	MAF (gnomAD)	Number of homozygous (gnomAD)
1	201180439	IGFN1	NM_001164586	c.6418G>A	p.(Ala2140Thr)	147660	0.001 (D)	0.138 (B)	0.0036	1
6	170871046	TBP	NM_003194	c.232_234del	p.(Gln95del)	600075			0	0
11	122722431	CRTAM	NM_019604	c.224A>G	p.(His75Arg)	612597	0.363 (T)	0.017 (B)	0.000036	0
11	125864848	CDON	NM_016952	c.2462G>A	p.(Arg821His)	608707	0.009 (D)	0.991 (D)	0.0006246	1
15	31521505	LOC283710	NM_001243538	c.75_76del					0.0001323	
16	11645607	LITAF	NM_001136473	c.431C>T	p.(Ser144Phe)	603795	0.00 (D)	0.071 (B)	0.0007910	2
20	43836872	SEMG1	NM_003007	c.934A>C	p.(Ser312Arg)	182140	0.085 (T)	0.02 (B)	0.002329	14
22	38122405	TRIOBP	NM_001039141	c.3842G>A	p.(Arg1281Lys)	609761	0.000 (D)	0.967 (D)	0	0
22	46345806	WNT7B	NM_058238	c.292C>T	p.(Arg98Ter)	601967			0	0
22	50589218	MOV10L1	NM_018995	c.2782G>T	p.(Ala928Ser)	605794	0.053 (T)	0.874 (d)	0.0001047	0
4	156135101	NPY2R	NM_000910	c.10A>G	p.(Ile4Val)	162642	0.94 (T)	0 (B)	0.00002	0

Polyphen-2 score: B: probably benign, D: probably damaging, d: possible damaging

Supplementary Table S4: ACMG classification of *WNT7B* (NM_058238.2) variations identified in this study

cDNA change	Protein change	MAF (GnomAD)	<i>In silico</i> predictions*	ACMG ¹ criteria	ACMG classification
c.225C>G	p.(Tyr75Ter)	0		<u>PVS1 Very Strong</u> <u>PS3 Strong</u> <u>PM2 Moderate</u>	Pathogenic
c.292C>T	p.(Arg98Ter)	0		<u>PVS1 Very Strong</u> <u>PS3 Strong</u> <u>PM2 Moderate</u>	Pathogenic
c.562G>A	p.(Gly188Ser)	0.0004%	11/12 pathogenic	<u>PS3 Strong</u> <u>PM2 Moderate</u> <u>PM3 Moderate</u> <u>PP3 Supporting</u>	Pathogenic

* Used tools : BayesDel_addAF, DANN, DEOGEN2, EIGEN, FATHMM-MKL, LIST-S2, M-CAP, MutationAssessor, MutationTaster, PrimateAI, SIFT, and MVP

- Richards S, Aziz N, Bale S, Bick D, Das S, Gastier-Foster J, Grody WW, Hegde M, Lyon E, Spector E, Voelkerding K, Rehm HL, Committee ALQA. Standards and guidelines for the interpretation of sequence variants: a joint consensus recommendation of the American College of Medical Genetics and Genomics and the Association for Molecular Pathology. *Genet Med* 2015;17(5):405-24

Supplementary Table S5: Main phenotypic features associated with *STRA6*, *RARB*, and *WNT7B* pathogenic variations

	<i>STRA6</i> ¹		<i>RARB</i> ^{2 3}		<i>WNT7B</i>	
	Features	%	Features	%	Features	%
Lung	Unilateral or bilateral Pulmonary agenesis Pulmonary hypoplasia Lobation defect Alveolar capillary dysplasia	40	Unilateral or bilateral Pulmonary hypoplasia	30	Bilateral Pulmonary agenesis Pulmonary hypoplasia	100
Diaphragm	Unilateral or bilateral Diaphragmatic hernia Diaphragmatic eventration	30	Unilateral or bilateral Diaphragmatic hernia Diaphragmatic eventration	60	Bilateral Diaphragmatic hernia Diaphragmatic eventration	≥ 50
Eye	Mostly bilateral Anophthalmia Microphthalmia Coloboma	~100	Mostly bilateral Anophthalmia Microphthalmia Coloboma Sclerocornea	~100	Microphthalmia Retinal dysplasia Coloboma	≥ 50
Heart	Conotruncal Defects Other heart defects	55	Patent ductus arteriosus Patent foramen ovale Peripheral pulmonic stenosis Left superior vena cava Atrial septal defects Ventral septal defects	45	Atrial septal defect Atrial septum defect Anomalous pulmonary venous drainage	≥ 50
Kidney	Pelvic kidney Horseshoe kidney Hydronephrosis Renal hypoplasia	25	None		Hypoplastic kidneys	≥ 50
Digestive system	Duodenal stenosis Pancreatic malformations	25	Malrotated bowel	20		
Genital system	Bicornuate uterus Uterine hypoplasia Cryptorchidism	15	Bicornuate uterus	rare		
Neurologic finding	Intellectual deficiency	50	Global developmental delay Variable language development Dystonia Chiari-I	~100 50 70		
Other	Splenic malformations Intrauterine growth retardation Thymic hypoplasia Subglottic laryngeal stenosis Cleft palate Corpus callosum anomaly Arhinencephaly Dandy–Walker malformation Spina bifida Hypoplastic nipples Hypoplastic toenails Polydactyly		Sagittal craniosynostosis Laryngomalacia		Choanal atresia Tracheo-laryngeal agenesis Abnormal trachea and main bronchi cartilage Small trachea-oesophageal fistula Skull bone softening	

The most frequent features are indicated in bold.

Plasiancie JC, N. "Microphthalmia 9 (PDAC). In: Erickson PRW-B, A.J., ed. Epstein's Inborn Errors of Development: The Molecular Basis of Clinical Disorders of Morphogenesis (3 ed), 2016.

Srour M, Caron V, Pearson T, Nielsen SB, Levesque S, Delrue MA, Becker TA, Hamdan FF, Kibar Z, Sattler SG, Schneider MC, Bitoun P, Chassaing N, Rosenfeld JA, Xia F, Desai S, Roeder E, Kimonis V, Schneider A, Littlejohn RO,

- 1
2
3 Douzgou S, Tremblay A, Michaud JL. Gain-of-Function Mutations in RARB Cause Intellectual Disability with
4 Progressive Motor Impairment. Hum Mutat 2016;**37**(8):786-93 doi: 10.1002/humu.23004.
5 3. Srour M, Chitayat D, Caron V, Chassaing N, Bitoun P, Patry L, Cordier MP, Capo-Chichi JM, Francannet C, Calvas P,
6 Ragge N, Dobrzeniecka S, Hamdan FF, Rouleau GA, Tremblay A, Michaud JL. Recessive and dominant mutations in
7 retinoic acid receptor beta in cases with microphthalmia and diaphragmatic hernia. Am J Hum Genet 2013;**93**(4):765-72
8
9
10
11
12
13
14
15
16
17
18
19
20
21
22
23
24
25
26
27
28
29
30
31
32
33
34
35
36
37
38
39
40
41
42
43
44
45
46
47
48
49
50
51
52
53
54
55
56
57
58
59
60

Confidential: For Review Only